

# Generation–Relaxation Algorithms to Construct Representative Atomistic Models of Amorphous Polymers: Influence of the Relaxation Method

David Curcó,<sup>\*,†</sup> Manuel Laso,<sup>‡</sup> and Carlos Alemán<sup>\*,§</sup>

*Departament d'Enginyeria Química, Facultat de Química, Universitat de Barcelona, Martí i Franques 1, Barcelona E-08028, Spain, Departamento de Ingeniería Química, E. T. S. de Ingenieros Industriales de Madrid, Universidad Politécnica de Madrid, José Gutiérrez Abascal 2, Madrid E-280006, Spain, and Departament d'Enginyeria Química, E.T.S. d'Enginyers Industrials de Barcelona, Universidad Politécnica de Catalunya, Diagonal 647, Barcelona E-08028, Spain*

*Received: September 7, 2004; In Final Form: October 13, 2004*

Two alternative methods to relax the atomistic models of amorphous polymers generated by structure simulation (SuSi), a procedure recently developed that combines a generation algorithm and a minimization algorithm to localize independent energy minima (*J. Chem. Phys.* **2003**, *119*, 2915), are presented. These relaxation methods, which are based on the geometric aspects of the conventional configurational bias (CB) and concerted rotation (ConRot) Monte Carlo techniques, have been compared with the minimization algorithm originally implemented in SuSi. For this purpose, we considered two polymeric systems: four polyethylene chains with each one containing 400 CH<sub>2</sub> groups and eight polyethylene chains with each one containing 800 CH<sub>2</sub> groups. The procedure based on ConRot has been demonstrated to be the most efficient of the three relaxation algorithms, while the minimization one is the least efficient. On the other hand, the method based on CB is limited by the difficulties to relax the interior segments of chain molecules.

## I. Introduction

The generation of representative, that is, equilibrated and relaxed, atomistic models of amorphous polymers is a very difficult task due to the high density and connectivity of these systems. However, since the pioneering work of Theodorou and Suter,<sup>1</sup> significant progress has been made in this field. Thus, in the past decades, a number of sophisticated methods, which are based on very different approaches, have been developed.<sup>2–12</sup>

Recently, we introduced a novel computational technique, which was denoted structure simulation (SuSi), for generating microstructures of amorphous polymers that avoids atomic overlaps and obeys the proper torsional distribution.<sup>11,12</sup> The method consists of a two-step procedure. First, microstructures are generated atom by atom using an algorithm that minimizes the energy associated with torsional degrees of freedom. The success of this algorithm resides both on the reduction of the radii of the atoms and on the consideration of the 1–4 interactions (those involving atoms separated by three chemical bonds) to choose the position of each generated atom. Second, the nonbonding interactions of the generated microstructures are relaxed using a minimization algorithm.

The generation algorithm implemented in SuSi proved to be very powerful and efficient, being able to produce atomistic models with minimum torsional strain using insignificant computational resources.<sup>11,12a</sup> On the other hand, although the minimization algorithm used to eliminate atomic overlaps is very efficient from a computational point of view, it presents some serious limitations.<sup>12</sup> First, the memory of the microstructure produced by the generation algorithm is not lost during the

process; that is, it hardly changes the overall conformational characteristics of the individual chains with respect to the starting microstructure. In addition, the effectiveness of the method is relatively low, with the improvement of the energy being usually lower than 10%.

In this work, the minimization algorithm used in SuSi has been replaced by geometric strategies based on the configurational bias<sup>13</sup> (CB) and concerted rotation<sup>14</sup> (ConRot) techniques. To examine and compare the effectiveness and efficiency of the new relaxation algorithms, we generate a number of microstructures of polyethylene and analyze the quality of the models after relaxation. These strategies are shown to contribute to a large extent to the success of SuSi.

In the next section, we initially summarize the basic elements of the generation algorithm of SuSi and, after this, we discuss the different relaxation strategies evaluated in this work. Section III compares the efficiency of the three relaxation strategies. For evaluation purposes, a united-atom representation for polyethylene (polybead) microstructures has been selected, since it is a useful and widely used benchmark system.

## II. SuSi: A Method for Generating Atomistic Models of Amorphous Polymers

**II.1. The Generation Algorithm.** To pack  $N$  polymer chains of  $n$  atoms each one in a box of fixed dimensions, that is, at a given density, inducing minimum torsional strain, the atomic radii ( $\{R\}$ ) are multiplied by a scale factor of  $\lambda < 1$ . The coordinates of the  $N \cdot n$  atoms of radii  $\{\lambda \cdot R\}$  are generated atom by atom and chain by chain. The generation of the first chain starts by selecting an arbitrary position within the simulation box. Excluding the first three atoms, whose relative positions are defined exclusively by geometric restrictions (bond distances and bond angles), a number of positions ( $k$ ) is randomly generated for the next atoms. In each case, the positions are

\* Authors to whom correspondence should be addressed. E-mail: curco@angel.qui.ub.es (D.C.); carlos.aleman@upc.es (C.A.).

<sup>†</sup> Universitat de Barcelona.

<sup>‡</sup> Universidad Politécnica de Madrid.

<sup>§</sup> Universidad Politécnica de Catalunya.

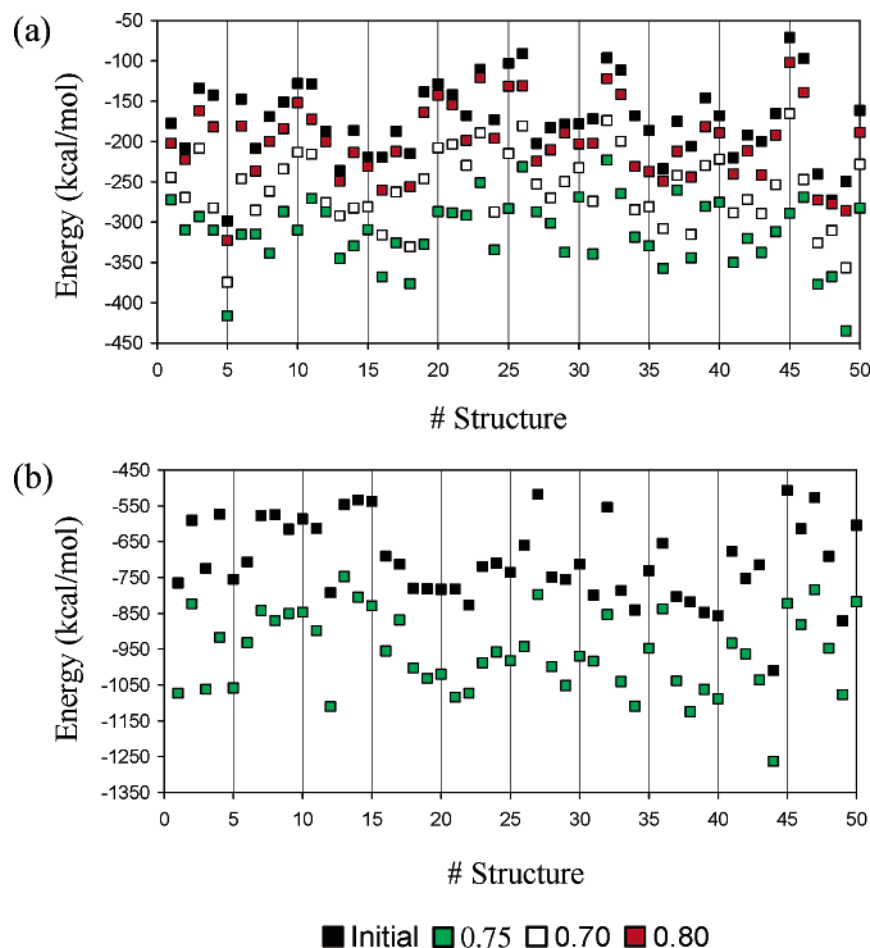


**Figure 1.** Comparison between the energies resulting from the generation algorithm (initial) and the energies obtained after  $2 \times 10^4$  steps of SuSi/CB relaxation for a set of 50 selected structures of PE4-400 (a) and PE8-800 (b). Relaxation of PE4-400 was performed considering  $\lambda_{CB} = 0.70, 0.75$ , and  $0.80$ , while  $\lambda_{CB} = 0.75$  was the only value used for PE8-800.

classified as *unfeasible* or *feasible* depending if atomic overlaps exist or not, respectively, with atoms previously generated and separated by more than three bonds. The coordinates of the new atoms are selected among the *j feasible* positions ( $j \leq k$ ) using a typical Monte Carlo criterion:

$$\text{Rnd}(1) < \frac{e^{-\tau E_j}}{e^{-\tau E_{j(\min)}}} \quad (1)$$

where  $E_j$  is the energy associated with the  $j$  position,  $\text{Rnd}(1)$  is a random number between 0 and 1, and  $\tau$  is a constant directly related to the probability of the positions in the criterion displayed in eq 1. The energy  $E_j$  is evaluated as the sum of the torsional and van der Waals contributions associated with the particles separated from  $j$  by three chemical bonds (1–4 interactions), that is, the van der Waals interaction between atoms  $j$  and  $j - 3$  and the torsional contribution involving the dihedrals defined by the bond between  $j - 1$  and  $j - 2$ . The omission of interactions different from 1–4 reduces notably the CPU effort, whereas at the same time a minimum torsional strain for the generated chain is guaranteed.

After the first chain has been successfully built, the remaining  $N - 1$  chains are generated using the same procedure. The only difference is the position used to start with such generation: an arbitrary position is chosen for the first chain, while for the remaining chains a nonfilled position is sought through a random search procedure.

**II.2. The Relaxation Algorithm.** The relaxation techniques evaluated in this work are based on the minimization, CB, and

ConRot methods, with the coupling to the generation algorithm described above being denoted SuSi/Min, SuSi/CB, and SuSi/ConRot, respectively. CB and ConRot are Monte Carlo sampling techniques<sup>13–15</sup> based on geometric algorithms able to efficiently modify the degrees of freedom of systems formed by long polymer chains, which are intractable by conventional simulation methods. It should be emphasized that our goal is to relax the microstructures provided by the generation algorithm and not to generate sequences of configurations through ergodic Monte Carlo simulations in the proper working ensemble. Accordingly, in this study, we have mainly concentrated on the geometric aspects of CB and ConRot. Generating such conformationally correct, relaxed configurations is an essential step in many molecular modeling techniques, for example, as initial guesses for MD or MC runs or for full minimization in amorphous cell calculations of linear elastic properties.

**Minimization.** A typical minimization algorithm was originally implemented in SuSi/Min. The method uses analytical expressions to determine the new position of the atoms and to correct such positions, ensuring that the internal geometry restrictions are satisfied.<sup>11</sup> The first step of the algorithm involves the calculation of  $(e_x, e_y, e_z)$  for each atom,  $i$ , using the following expression:

$$e_q(i) = \sum_{j \neq i} E_{ij} u_q(i \rightarrow j) \quad \text{with } q = x, y, \text{ and } z \quad (2)$$

where  $E_{ij}$  is the interaction energy between atoms  $i$  and  $j$  and  $(u_x, u_y, u_z)$  is the unit vector that connects atoms  $i$  and  $j$ . Then,

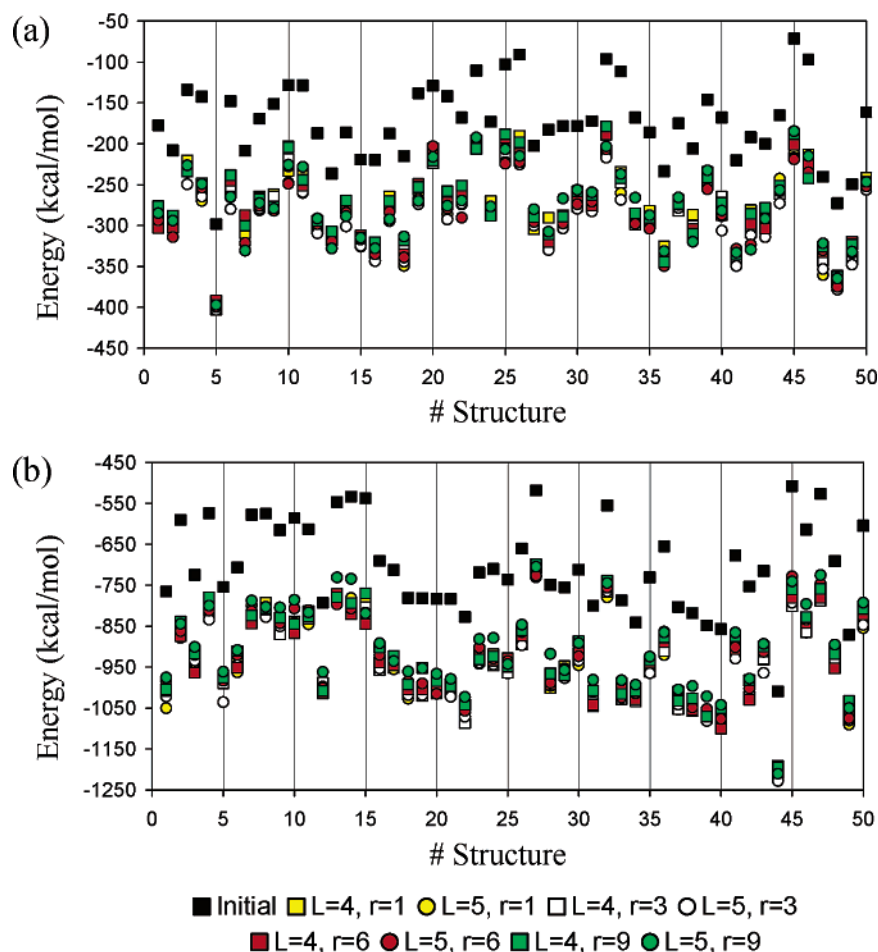


**Figure 2.** Comparison between the energies resulting from the generation algorithm (initial) and the energies obtained after  $2 \times 10^4$  steps of SuSi/ConRot relaxation for a set of 50 selected structures of PE4-400 (a) and PE8-800 (b). Relaxations were performed using different combinations of  $L = 4$  and 5 and  $r = 1, 3, 6$ , and  $9^\circ$ .

the position of atom  $i$  is changed from  $(x_i, y_i, z_i)$  to  $(x'_i, y'_i, z'_i)$  as follows:

$$q(i)' = q(i) + e_q(i)\Delta \quad \text{with } q = x, y, \text{ and } z \quad (3)$$

where  $\Delta$  is a constant initially specified by the user. The relaxation is considered as converged when after several trials the energy obtained for the new positions does not improve with respect to that provided by the last accepted position. The efficiency of the minimization procedure was improved using a double cutoff strategy for the evaluation of the interaction energies: the cutoff is increased after some minimization steps. More technical details about this minimization method were provided in ref 11.

**Configurational Bias.** In the CB method, a randomly selected polymer chain is cut at an arbitrary position and sequentially rebuilt bond by bond.<sup>13</sup> For each bond to be appended, a set of  $M$  torsional angles is randomly chosen between 0 and  $2\pi$ , with the coordinates of all atoms that are dependent on the actual torsional angle being computed. After this, the energy associated with each of the  $M$  positions is evaluated. To increase the efficiency of the relaxation, only the 1–4 interactions, as in the generation algorithm, are taken into account to evaluate these energies. One of the positions is randomly chosen with a probability proportional to its Boltzmann weight. Obviously, in the CB method, it is not possible to choose directly the lowest energy position, since a successful reconstruction of the chain using the lowest energy path, that is, the lowest energy position

for each rebuilt bond, is very improbable. On the other hand, application of this adapted CB algorithm to the relaxation of the generated structures has shown that the effectiveness of the relaxation improves considerably when the atomic radii used in the reconstruction of the chain are multiplied by a scale factor of  $\lambda_{CB} < 1$ , even though the unscaled radii are employed for energy evaluations. The scale factor  $\lambda_{CB}$  is not necessarily identical to that used in the generation algorithm.

**Concerted Rotation.** In ConRot, a chain is selected at random and a site at an arbitrary position,  $i$ , along its backbone is also selected. Next,  $L$  consecutive atoms of the main chain (in this work,  $L = 4$  or 5) are deleted. Then, the ConRot geometric algorithm joins the two segments of the interrupted polymer chain by rebuilding the positions for the  $L$  deleted atoms. The initial positions of some of the deleted atoms are used in the ConRot move as auxiliary variables when rebuilding the deleted part of the backbone. The exact procedure used to do this depends on the value of  $L$ .

For  $L = 4$ :

- (i) The dihedral angle formed by atoms  $i - 2$ ,  $i - 1$ , and  $i$ , whose coordinates remain fixed, and the first deleted atom, that is, atom  $i + 1$ , are changed from their initial values by adding a random number chosen between  $+r$  and  $-r$ .
- (ii) The position of the other three deleted atoms, that is, atoms  $i + 2$ ,  $i + 3$ , and  $i + 4$ , is determined by numerically solving the bond length and bond angle constraints imposed by the fixed geometry of the chain.

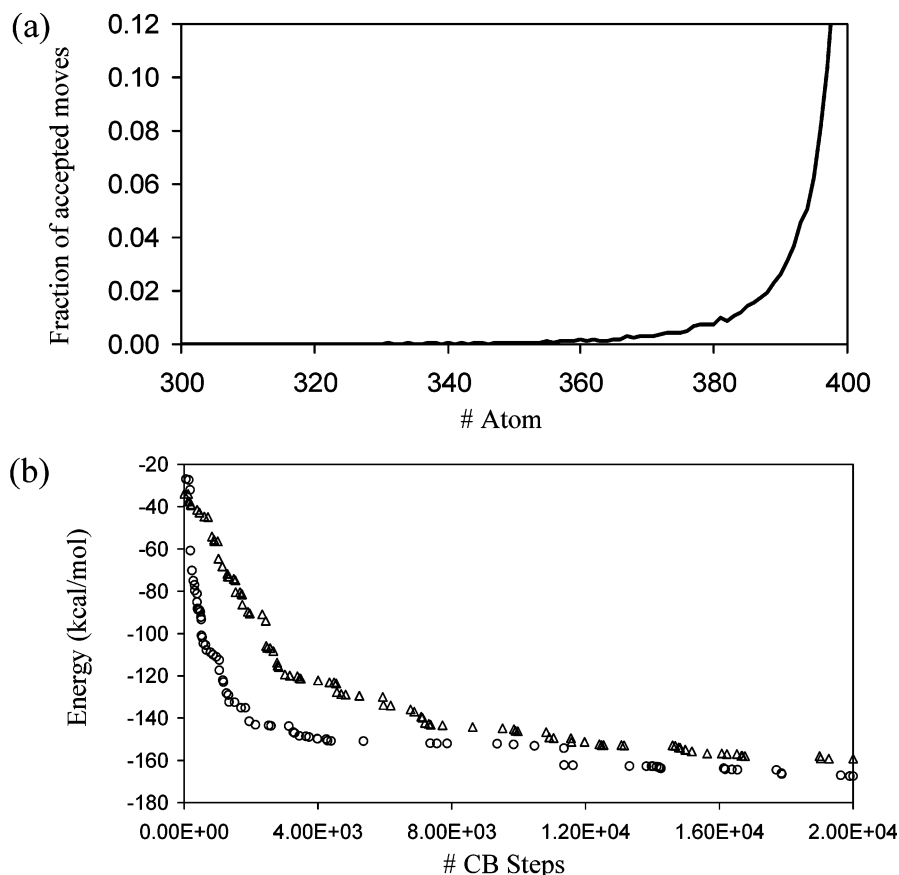


**Figure 3.** Fraction of accepted CB moves in the last 100 atoms of the chain for a selected structure of PE4-400 (a). Variation of the energy against the number of CB steps for two selected structures of PE4-400 (b).

Thus, only one of the seven dihedral angles involved in a move with  $L = 4$  is considered as an independent variable, with the rest being imposed by the internal geometry of the system.

For  $L = 5$ :

(i) This step is identical to that discussed above for  $L = 4$ : the dihedral angle formed by atoms  $i - 2$ ,  $i - 1$ ,  $i$ , and  $i + 1$  changes by adding a random number chosen between  $+r$  and  $-r$ .

(ii) Considering the original position of atom  $i + 2$ , its coordinates are readjusted to fulfill the bond length and bond angle with atoms  $i + 1$  and  $i$ . After this, the dihedral angle formed by atoms  $i - 1$ ,  $i$ ,  $i + 1$ , and  $i + 2$  is moved by adding a new random number again chosen between  $+\alpha$  and  $-\alpha$ .

(iii) The positions of atoms  $i + 3$ ,  $i + 4$ , and  $i + 5$  are determined numerically to fulfill the internal geometry constraints.

Accordingly, for  $L = 5$ , the number of dihedral angles used as independent variables is two. The cases  $L = 4$  and  $L = 5$  correspond to the standard ConRot and extended ConRot (ECROT) moves,<sup>14</sup> respectively, where one (ConRot) or two (ECROT) driver angles are used.

**II.3. The Force Field.** Polymer chains consist of  $N \cdot n$  atoms or pseudoatoms connected by rigid bonds and fixed bond angles. The intramolecular interactions of atoms/pseudoatoms separated by four or more bonds and all the intermolecular interactions constitute the set of nonbonded interactions, which are represented by pairwise additive Lennard-Jones 12-6 and Coulombic electrostatic potentials:

$$E_{ij}^{\text{LJ}} = \frac{A_{ij}}{r_{ij}^{12}} - \frac{B_{ij}}{r_{ij}^6} \quad (4)$$

$$E_{ij}^{\text{Coul}} = \frac{q_i q_j}{4\pi\epsilon_0 r_{ij}} \quad (5)$$

where the parameters  $A_{ij}$  and  $B_{ij}$  correspond to  $(\epsilon_i \epsilon_j)^{1/2} (R_i + R_j)^{12}$  and  $2(\epsilon_i \epsilon_j)^{1/2} (R_i + R_j)^6$ , respectively, and  $R_i$  and  $\epsilon_i$  are the van der Waals parameters of site  $i$ . It should be emphasized that, although the Coulombic expression is included in the force field, no electrostatic interaction was considered in this study for polyethylene. However, it should be remarked that such interactions are important for polar polymers such as nylons.<sup>12b</sup> Associated with each dihedral angle ( $\varphi$ ) is also a torsional potential of the following form:

$$E_{\text{tor}} = \sum_{n=1}^3 \frac{V_n}{2} [1 + \cos(n\varphi - \gamma_n)] \quad (6)$$

where  $V_n$  is a force constant,  $n$  is the multiplicity factor, and  $\gamma_n$  is the phase angle. A scale factor of 0.5 is applied to reduce all the nonbonding interactions within atoms of the same chain separated by exactly three bonds (1-4 interactions). The scaling of 1-4 interactions is consistent with the analytical energy expressions showed above and the potential energy parameters of the Amber force field.<sup>16</sup>

The polyethylene chains studied in this work consist of  $\text{CH}_2$  pseudoatoms ( $\text{CH}_3$  at the chain ends) connected by rigid bonds and angles:  $d(\text{CH}_2-\text{CH}_2) = d(\text{CH}_2-\text{CH}_3) = 1.526 \text{ \AA}$  and  $\angle\text{CH}_2-\text{CH}_2-\text{CH}_2 = \angle\text{CH}_2-\text{CH}_2-\text{CH}_3 = 112.4^\circ$ . The torsion about  $\text{CH}_2-\text{CH}_2$  and  $\text{CH}_2-\text{CH}_3$  bonds was described using the following parameters:  $V_3 = 2 \text{ kcal/mol}$  and  $\gamma = 0^\circ$ . Finally, the Lennard-Jones parameters of  $\text{CH}_2$  and  $\text{CH}_3$  pseudoatoms are  $r(\text{CH}_2) = 1.925 \text{ \AA}$ ,  $r(\text{CH}_3) = 2.00 \text{ \AA}$ ,  $\epsilon(\text{CH}_2) = 0.12 \text{ kcal/}$

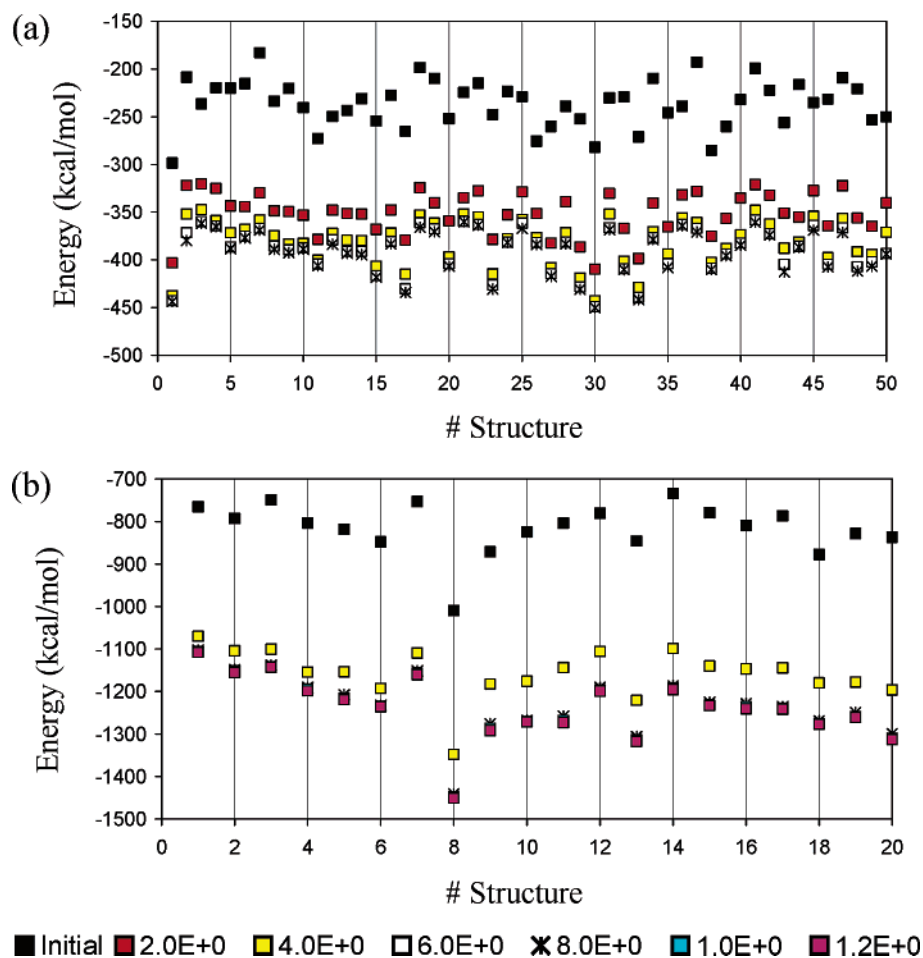


**Figure 4.** Variation of the energy against the number of relaxation steps using SuSi/ConRot for a set of 50 selected structures of PE4-400 (a) and PE8-800 (b).

mol, and  $\epsilon(\text{CH}_3) = 0.15$  kcal/mol. All these parameters were taken from the united-atom parametrization of the Amber force field.<sup>16</sup>

### III. Results and Comparison of SuSi/Min, SuSi/CB, and SuSi/ConRot

We have compared the efficiencies of the three relaxation algorithms discussed above by carrying out calculations on two different types of amorphous polyethylene, which differ among them in the number of polymer chains ( $N$ ) and the number of  $\text{CH}_2$  units ( $n$ ). These systems are formed by (i)  $N = 4$  and  $n = 400$  (PE4-400) and (ii)  $N = 8$  and  $n = 800$  (PE8-800). The number of structures generated was 200 for PE-400 and 100 for PE8-800, with the parameters used in the generation being  $\lambda = 0.75$  and  $k = 20$  for the two systems.

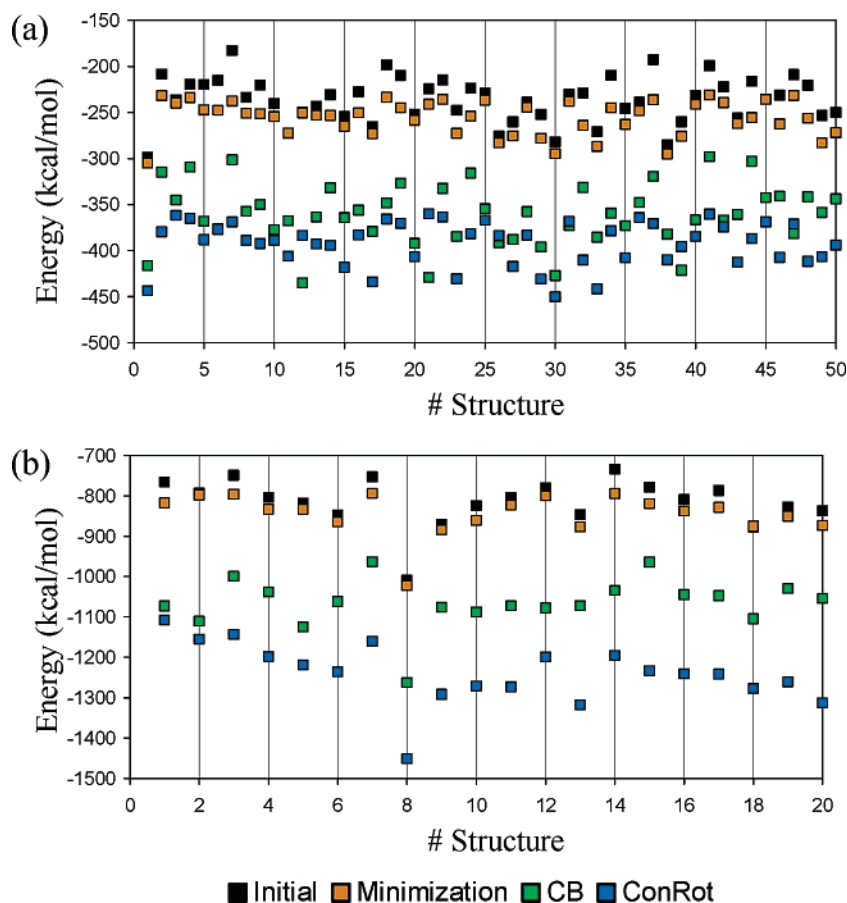
To check the influence of some relevant parameters on the effectiveness of the adapted CB and ConRot geometric algorithms, the generated structures were relaxed with SuSi/CB considering  $\lambda_{\text{CB}} = 0.70, 0.75$ , and  $0.80$  and with SuSi/ConRot considering  $L = 4$  and  $5$  and  $r = 1, 3, 6$ , and  $9^\circ$ . Results are displayed in Figures 1 and 2 for a set of 50 representative structures (results for the whole set of structures are provided as Supporting Information), where the energies of the generated structures are compared with the energies obtained after  $2 \times 10^4$  steps of SuSi/CB and SuSi/ConRot relaxation, respectively.

Figure 1a shows that the best results for PE4-400 are obtained systematically when the scale factors used in the generation and CB relaxation algorithms are equal, that is,  $\lambda = \lambda_{\text{CB}} = 0.75$ . The energies obtained using  $\lambda_{\text{CB}} = 0.75$  during the relaxation

are on average lower than the energies provided using  $\lambda_{\text{CB}} = 0.70$  and  $0.80$  by 59 and 115 kcal/mol, respectively. Furthermore, the lowest energy structure was also obtained with  $\lambda_{\text{CB}} = 0.75$ , with the structures relaxed with  $\lambda_{\text{CB}} = 0.70$  and  $0.80$  being at least 60 and 113 kcal/mol, respectively, less stable.

One of the major drawbacks of SuSi/CB is the poor computational efficiency of the CB algorithm during the relaxation. Thus, a huge amount of computational resources are needed to relax each structure, since the acceptance rates are very low. This must be attributed to the difficulties in the reconstruction of the central part of the molecule. Not surprisingly, the successful reconstruction of the molecule is extremely difficult when it starts from an atom far from the end, since a very large number of consecutive accepted moves are required. This is illustrated in Figure 3a, which shows the fraction of accepted moves for the last 100 atoms of the chain in PE4-400. As can be seen, the effectiveness of the CB algorithm increases when the distance to the end of the chain decreases, being clearly negligible in the middle of the chain. This approximately exponential decay of the efficiency of CB moves with the depth of the cut renders CB useless for chains longer than about 40–50  $\text{CH}_2$  groups. On the other hand, the energy of PE4-400 is roughly converged after  $2 \times 10^4$  steps of CB relaxation. Thus, the energy reached for the whole system after  $1.2 \times 10^4$  CB steps is hardly reduced by additional relaxation. This is illustrated in Figure 3b, which shows the variation of the energy against the number of CB steps for two randomly chosen structures of PE4-400.





**Figure 5.** Comparison between the energies resulting from the generation algorithm (initial) and the energies obtained after relaxation using SuSi/Min, SuSi/CB, and SuSi/ConRot for a set of 50 selected structures of PE4-400 (a) and PE8-800 (b).

According to the result obtained for PE4-400, we decided to relax the structures generated for PE8-800 using only  $\lambda_{CB} = 0.75$ . Results after  $2 \times 10^4$  steps of SuSi/CB are displayed in Figure 1b. It is worth noting that the reduction of energy was on average 259 kcal/mol, this value being similar to that obtained for PE4-400. Furthermore, analyses of the results do not provide additional information with respect to that obtained for PE-400: the effectiveness of the CB algorithm is negligible for the atoms separated by 19 or more bonds from the end of the chain and the energy is approximately converged after  $2 \times 10^4$  steps of relaxation, with the latter being a consequence of the former.

Regarding SuSi/ConRot, results obtained after  $2 \times 10^4$  steps of relaxation using  $L = 4$  and 5 and  $r = 1, 3, 6$ , and  $9^\circ$  are displayed in Figure 2. For PE4-400, the energy decreases on average 101 and 113 kcal/mol during relaxation with  $L = 4$  and 5, respectively, while, for PE8-800, the reduction produced by  $L = 4$  and 5 is 232 and 237 kcal/mol, respectively. These results indicate that when two dihedral angles are used as independent variables better results are systematically obtained. Furthermore, for both  $L = 4$  and 5, the maximum relaxation was obtained on average for  $r = 3^\circ$ . Thus, the efficiency of the relaxation procedure does not improve when the variation of the atomic coordinates between two successive steps is very large. Indeed, moderate changes in the atomic coordinates produce the best results.

On the other hand, the relaxation of the structures is not completed after  $2 \times 10^4$  steps. According to this feature and the results displayed in Figure 2, we decided to continue the process of relaxation until the equilibration of the energy using  $L = 5$  and  $r = 3^\circ$ . For this purpose, we selected 50 and 25

structures of lower energy for PE4-400 and PE8-800, respectively. Figure 4 shows the evolution of the energy against the number of ConRot steps. As can be deduced by the overlap of the symbols, the structures of PE4-400 are converged after  $6 \times 10^4$  steps, while those of PE8-800 require  $1.0 \times 10^5$  steps. Furthermore, the results displayed in Figure 4 reveal that the greatest effectiveness of SuSi/ConRot is achieved during the first steps of relaxation. Thus, for PE4-400 and PE8-800, the reduction of the energy with respect to the initial value is on average 61 and 42%, respectively, after  $4 \times 10^4$  steps of relaxation. These values are 66 and 52% at the end of the relaxation, indicating that, for PE-400 and PE8-800, the last  $4 \times 10^4$  and  $8 \times 10^4$  steps provide an improvement of only 5 and 10%, respectively.

Figure 5 compares the energies obtained using SuSi/Min, SuSi/CB, and SuSi/ConRot for the 50 and 20 structures of PE-400 and PE8-800, selected above. As can be seen, SuSi/ConRot provides in all cases the structures of lowest energy. This is a very reasonable result, since, as was discussed previously, the effectiveness of CB is low for the interior segments of the chain molecules. Furthermore, SuSi/ConRot is several orders of magnitude more efficient than SuSi/CB, since the rate of accepted moves is considerably higher for the former than for the latter. On the other hand, the energies provided by SuSi/CB and SuSi/ConRot are considerably smaller than those derived from SuSi/Min, pointing out the limitations associated to the relaxation of amorphous polymers through simple minimization algorithms.

To examine the influence of the relaxation algorithm on the resulting microstructures, we have evaluated different static amorphous state properties. Figure 6 shows a comparison

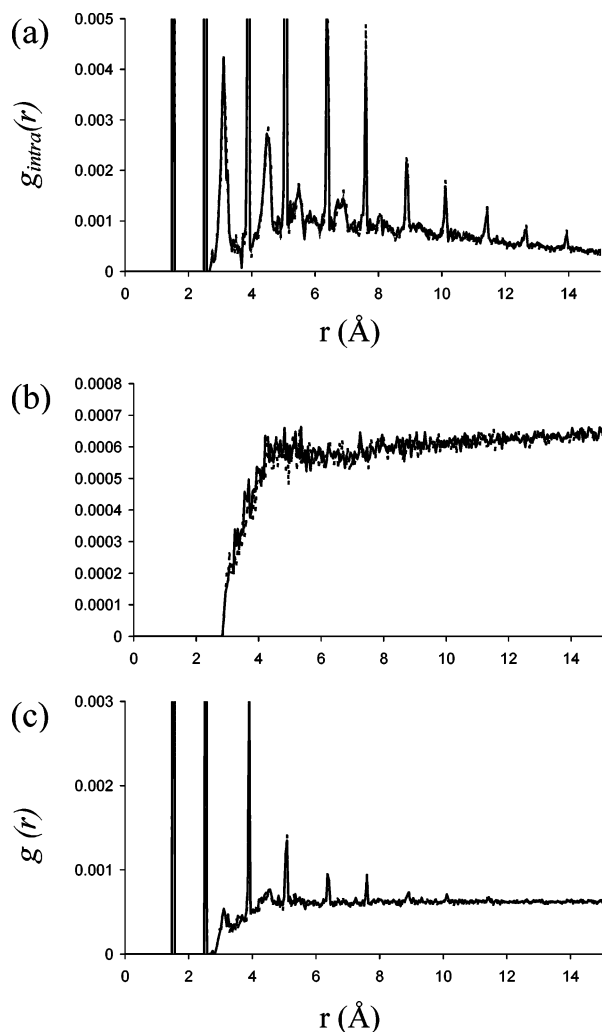


**Figure 6.**  $\text{CH}_2 \cdots \text{CH}_2$  intramolecular (a), intermolecular (b), and total (c) radial distribution functions of PE4-400 calculated using the structures relaxed with SuSi/ConRot (solid line) and SuSi/CB (dotted line).

between the intramolecular, intermolecular, and total  $\text{CH}_2 \cdots \text{CH}_2$  radial distribution functions for PE4-400 obtained from SuSi/CB and SuSi/ConRot structures. The agreement between the structures provided by the two relaxation algorithms is excellent. Figure 7 compares for PE8-800 the torsion angle distribution of the polymer chains obtained with SuSi/CB and SuSi/ConRot. The radial distribution functions of PE8-800 and the distribution of dihedral angles obtained for PE4-400 are very similar to those

**TABLE 1: Cohesive Energy ( $E_{\text{coh}}$ ) and Hildebrand Solubility Parameter<sup>a</sup> ( $\delta$ ) Calculated for PE4-400 and PE8-800**

system	method	$E_{\text{coh}}$ (kcal/mol·CRU <sup>a</sup> )	$\delta$ (cal/cm <sup>3</sup> ) <sup>1/2</sup>
PE4-400	SuSi/Min	−0.91	7.4
	SuSi/CB	−1.01	7.8
	SuSi/ConRot	−1.16	8.4
PE8-800	SuSi/Min	−0.89	7.3
	SuSi/CB	−0.99	7.7
	SuSi/ConRot	−1.12	8.2

<sup>a</sup> The experimental value of  $\delta$  is 7.8 cal/cm<sup>3</sup> (ref 17). <sup>b</sup> CRU: chemical repeating unit.

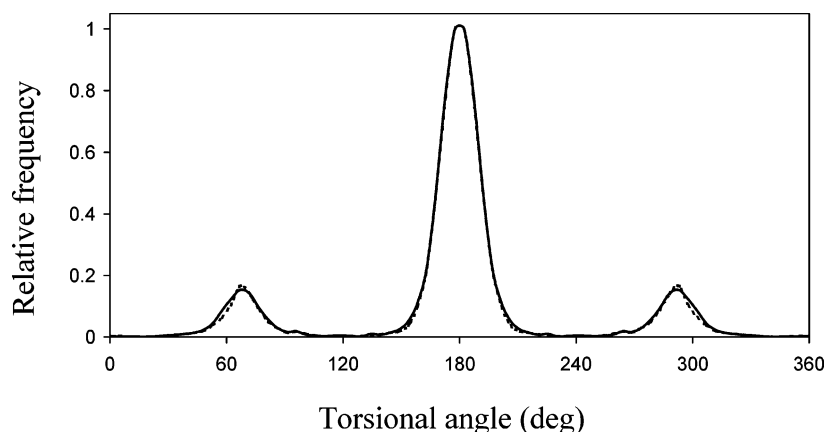
displayed in Figures 6 and 7, respectively. As can be seen, there is excellent agreement between the structures provided by the two relaxation methods, suggesting that the generation algorithm is the main one responsible for the structural properties. Consistently, the results provided by SuSi/Min are also very similar to those displayed in Figures 6 and 7.

Table 1 lists for PE4-400 and PE8-800 the cohesive energy ( $E_{\text{coh}}$ ), which is defined as the increase in energy per mole of chemical repeating unit (CRU) of material if all the intermolecular forces are eliminated, and the Hildebrand solubility parameter ( $\delta$ ) calculated as the square root of  $-E_{\text{coh}}$  referred to a unit volume of material. The highest value of  $\delta$  was obtained using the structures relaxed with ConRot, with the values derived from SuSi/CB and SuSi/Min being 0.6 and 1.0 cal/cm<sup>3</sup> smaller, respectively. The agreement of the SuSi/CB and SuSi/ConRot values with the experimental estimation (7.8 cal/cm<sup>3</sup>)<sup>17</sup> is very remarkable. The small discrepancies between the theoretical and experimental values must be attributed to the force-field parameters used to simulate polyethylene. These were taken from Amber, a widely used force field which was initially designed to study biological macromolecules (proteins and nucleic acids).<sup>16</sup>

Table 2 compares the estimated solubility coefficients ( $S$ ) of small gas penetrants (He, Ar, and N<sub>2</sub>) in PE4-400 and PE8-800 with experimental values for amorphous polyethylene.<sup>18</sup> The values of  $S$  of the penetrant  $i$  were calculated in the usual way:

$$S_i = \left( \frac{T_0}{TP_0} \right) e^{-\mu_i^{\text{ex}}/RT} \quad (7)$$

where  $T_0 = 273.15$  K,  $T$  is the temperature of the system (298 K),  $P_0 = 1.013$  bar, and  $\mu_i^{\text{ex}}$  is the infinite-dilution excess chemical potential of the penetrant  $i$  sorbed in the relaxed microstructures. The value of  $\mu_i^{\text{ex}}$  for He, Ar, and N<sub>2</sub> was computed using the Widom insertion method.<sup>19</sup> The van der



**Figure 7.** Torsion angle distribution for PE8-800 using the structures relaxed with SuSi/ConRot (solid line) and SuSi/CB (dotted line).

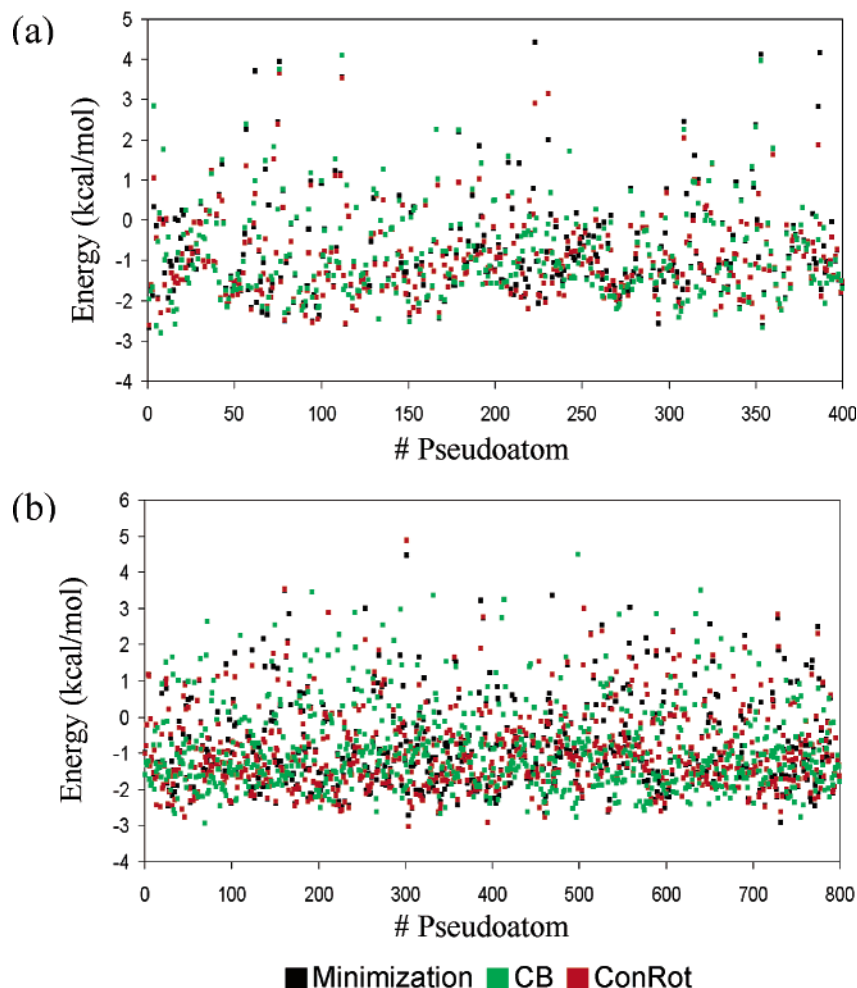


**Figure 8.** Nonbonding energy associated to each pseudoatom of the chain for the structures of PE4-400 (a) and PE8-800 (b) obtained using SuSi/Min, SuSi/CB, and SuSi/ConRot.

**TABLE 2: Solubility for Several Penetrants [ $\text{cm}^3(\text{STP})/\text{cm}^3\cdot\text{bar}$ ] in PE4-400 and PE8-800 at 298 K<sup>a</sup>**

system	method	He	Ar	N <sub>2</sub>
PE4-400	SuSi/Min	0.065	0.289	0.208
	SuSi/CB	0.053	0.241	0.163
	SuSi/ConRot	0.059	0.272	0.194
PE8-800	SuSi/Min	0.064	0.286	0.204
	SuSi/CB	0.058	0.269	0.196
	SuSi/ConRot	0.056	0.272	0.195
amorphous polyethylene	experimental <sup>b</sup>	0.012	0.103	0.041

<sup>a</sup> Experimental values for amorphous polyethylene are also included.

<sup>b</sup> From ref 18.

Waals parameters given by van der Vegt et al.<sup>20</sup> were used for the penetrants, which were being described as simple spheres. As can be seen, the  $S$  values obtained for the structures relaxed with the minimization algorithm are slightly higher than those achieved using the structures relaxed with CB and ConRot. However, the most remarkable feature is that the coefficients derived from SuSi/Min, SuSi/CB, and SuSi/ConRot microstructures are, in all cases, in excellent agreement with experimental data. This good accordance demonstrates the relevance of the structures provided by the computational strategies described in this work.

The results obtained for PE4-400 and PE8-800 strongly suggest that, even though ConRot is more effective than CB, the influence of the method used for relaxation on the structural properties is minor. This is because the variation of the atomic coordinates produced by these two algorithms is in general

small: on average, 0.186 and 0.178 Å/atom for PE4-400 and PE8-800, respectively. Accordingly, ConRot and CB relaxations minimize the unfavorable contacts (major overlaps) of the structures constructed by the generation algorithm but they do not induce drastic conformational changes through large variations in the dihedral angles. Conversely, the efficiency of the method used to minimize unfavorable nonbonding interactions has a large impact on energy-related properties, like  $\delta$ . This influence is clearly illustrated in Figure 8, which shows for PE4-400 and PE8-800 the nonbonding energy associated to each pseudoatom of the chain for the structures obtained using SuSi/Min, SuSi/CB, and SuSi/ConRot. As can be seen, such energies strongly depend on the relaxation algorithm, being in general more favorable for the structures provided by SuSi/ConRot.

#### IV. Conclusions

We described and analyzed several strategies for relaxing the atomistic models of amorphous polymers generated by SuSi. Calculations on two polymeric systems formed by polyethylene chains indicated that SuSi/ConRot and SuSi/Min are the most and least effective methods, respectively, while SuSi/CB is limited by the difficulties to relax the interior segments of the chains. It should be noted that the efficiency of the SuSi/ConRot and SuSi/CB methods with respect to SuSi/Min is probably related to the ability of the former methods to sample the configurational space.

Examination of the relaxed structures for PE4-400 and PE8-800 indicated that the influence of the relaxation algorithm on



the large-scale structural properties of the polymer chains is almost negligible. This is because relaxation algorithms act on the unfavorable nonbonding interactions, which result from a few overlaps and which are minimized by applying very small changes in the atomic coordinates. Thus, the relaxation procedures are not able to induce conformational changes on the chains due to the polymeric nature of the systems, that is, a relatively dense packing of long chains. Conversely, the effectiveness of the method used for the relaxation affects considerably the energy-related properties. Accordingly, the values of  $E_{\text{coh}}$  and  $\delta$  provided by the different relaxation methods differ by more than 0.2 kcal/mol·CRU and 1 (cal/cm<sup>3</sup>)<sup>1/2</sup>, respectively.

Another point that deserves special consideration is that the energy after relaxation depends on the energy before relaxation. Thus, starting structures of low energy systematically lead to relaxed structures of low energy, even though the range of variation of the energies for a given set of structures is smaller after rather than before relaxation. Furthermore, the two steps involved in SuSi/ConRot represent opposite computational extremes: the efficiency of the generation algorithm is very high, while the relaxation requires a notable computational effort. The whole of these features suggests that a good strategy for modeling amorphous polymers consists of the generation of a very large number of structures, their subsequent categorization in terms of energies, and the relaxation of only those with an energy lower than a certain cutoff.

**Acknowledgment.** We are indebted to CESCA (Centre de Supercomputació de Catalunya) and CEPBA (Centre Europeu de Paral·lelisme de Barcelona) for computational facilities. This work was supported by MCYT and FEDER with Grant MAT2003-00251.

**Supporting Information Available:** Figures showing comparisons between the energies resulting from the generation algorithm and the energies obtained after  $2 \times 10^4$  steps of SuSi/CB and SuSi/ConRot relaxation for the structures of PE4-400 and PE8-800. This material is available free of charge via the Internet at <http://pubs.acs.org>.

## References and Notes

- (1) (a) Theodorou, D. N.; Suter, U. W. *Macromolecules* **1985**, *18*, 1467. (b) Theodorou, D. N.; Suter, U. W. *Macromolecules* **1986**, *19*, 139.
- (2) (a) Clarke, J. H. R.; Brown, D. *Mol. Simul.* **1989**, *19*, 139. (b) Rapold, R. F.; Suter, U. W. *Macromol. Theory Simul.* **1994**, *3*, 1.
- (3) (a) McKechnie, J. I.; Brown, D.; Clarke, J. H. R. *Macromolecules* **1992**, *25*, 1562. (b) Gusev, A. A.; Zehnder, M. M.; Suter, U. W. *Macromolecules* **1994**, *27*, 615. (c) Brown, D.; Clarke, J. H. R.; Okuda, M.; Yamazaki, T. J. *J. Chem. Phys.* **1994**, *100*, 6011.
- (4) (a) Müller, M.; Nievergelt, J.; Santos, S.; Suter, U. W. *J. Chem. Phys.* **2001**, *114*, 9764. (b) Santos, S.; Suter, U. W.; Müller, M.; Nievergelt, J. *J. Chem. Phys.* **2001**, *114*, 9772.
- (5) Khare, R.; Paulaitis, M. E.; Lustig, S. R. *Macromolecules* **1993**, *26*, 7203.
- (6) (a) Rapold, R. F.; Mattice, W. L. *J. Chem. Soc., Faraday Trans.* **1995**, *91*, 2435. (b) Rapold, R. F.; Mattice, W. L. *Macromolecules* **1996**, *29*, 2457. (c) Cho, J.; Mattice, W. L. *Macromolecules* **1997**, *30*, 637. (d) Clancy, T. C.; Mattice, W. L. *J. Chem. Phys.* **2000**, *112*, 49.
- (7) Li, Y.; Mattice, W. L. *Macromolecules* **1992**, *25*, 4942.
- (8) (a) Pant, P. V. K.; Theodorou, D. N. *Macromolecules* **1995**, *28*, 7224. (b) Mavrantzas, V. G.; Boone, T. D.; Zervopoulou, E.; Theodorou, D. N. *Macromolecules* **1999**, *32*, 5072.
- (9) (a) Curro, J. G.; Schweizer, K. S. *J. Chem. Phys.* **1989**, *91*, 5059. (b) Schweizer, K. S.; Curro, J. G. *Adv. Polym. Sci.* **1994**, *116*, 319.
- (10) Uhlherr, A.; Mavrantzas, V. G.; Doxastakis, M.; Theodorou, D. N. *Macromolecules* **2001**, *34*, 8554.
- (11) Curc6, D.; Alemán, C. *J. Chem. Phys.* **2003**, *119*, 2915.
- (12) (a) Curc6, D.; Alemán, C. *J. Comput. Chem.* **2004**, *25*, 790. (b) Alemán, C.; Curc6, D. *Macromol. Theory Simul.* **2004**, *13*, 345.
- (13) (a) Siepmann, J. I. *Mol. Phys.* **1990**, *70*, 1145. (b) Siepmann, J. I.; Frenkel, D. *Mol. Phys.* **1992**, *75*, 59. (c) de Pablo, J. J.; Laso, M.; Suter, U. W. *J. Chem. Phys.* **1992**, *96*, 2395.
- (14) (a) Dodd, L. R.; Boone, T. D.; Theodorou, D. N. *Mol. Phys.* **1993**, *78*, 961. (b) Leontidis, E.; de Pablo, J. J.; Laso, M.; Suter, U. W. *Adv. Polym. Sci.* **1994**, *116*, 283.
- (15) Leontidis, E.; Forrest, B. M.; Widmann, A. H.; Suter, U. W. *J. Chem. Soc., Faraday Trans.* **1995**, *91*, 2355.
- (16) Weiner, S. J.; Kollman, P. A.; Nguyen, D. T.; Case, D. A. *J. Comput. Chem.* **1986**, *7*, 230.
- (17) van Krevelen, D. V. *Properties of polymers, their estimation and correlation with chemical structure*; Elsevier: Amsterdam, The Netherlands, 1976.
- (18) Michaels, A. S.; Bixler, H. J. *J. Polym. Sci.* **1961**, *50*, 393.
- (19) (a) Widom, B. *J. Phys. Chem.* **1982**, *86*, 869. (b) Widom, B. *J. Chem. Phys.* **1963**, *39*, 2808.
- (20) van der Vegt, N. F. A.; Briels, W. J.; Wessling, M.; Strathmann, H. *J. Chem. Phys.* **1996**, *105*, 8849.